Article

Cell Reports

Genetic Dissection of the Impact of miR-33a and miR-33b during the Progression of Atherosclerosis

Graphical Abstract

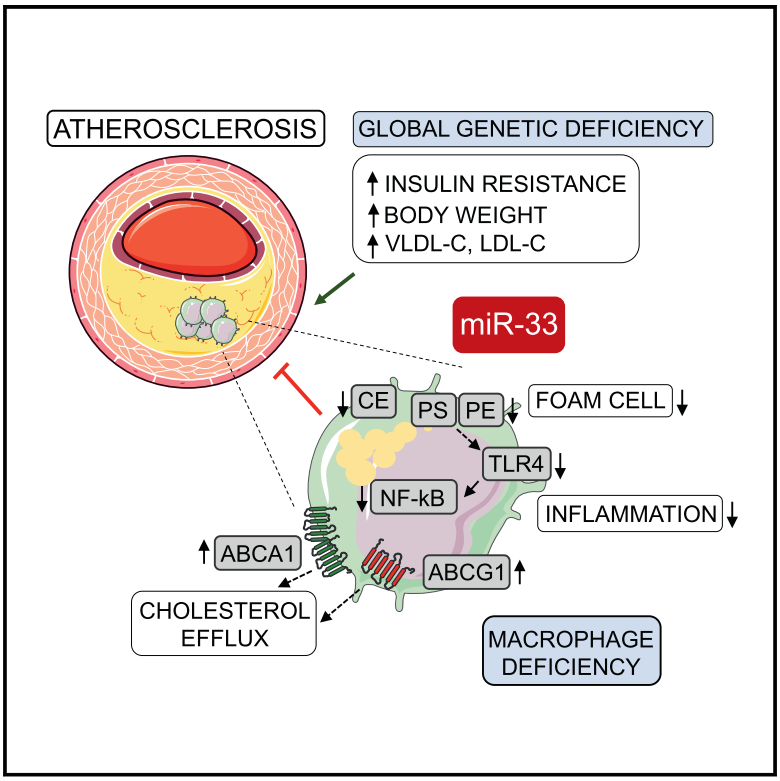

Authors

Nathan L. Price, Noemi Rotllan, Alberto Canfrán-Duque, ..., Ángel Baldán, Yajaira Suárez, Carlos Fernández-Hernando

Correspondence

carlos.fernandez@yale.edu

In Brief

miR-33a and miR-33b, the miR-33 family of miRNAs, are important regulators of reverse cholesterol transport and atherosclerosis. Price et al. have developed genetic models to explore the specific roles of miR-33a and miR-33b in atherosclerotic plaque formation. Their findings highlight both the utility and potential issues involved in anti-miR-33 therapies.

Highlights

- In vivo, *miR-33*$^{-/-}$ macrophages have ↑ cholesterol efflux and ↓ lipid accumulation
- Transplant with miR-33-deficient bone marrow decreased plaque size and lipid deposition
- Transplant with bone marrow from *miR-33b*^{KI} mice does not impact plaque formation
- Whole-body loss of miR-33 results in dyslipidemia, obesity, and insulin resistance

Price et al., 2017, Cell Reports *21*, 1317–1330
October 31, 2017
https://doi.org/10.1016/j.celrep.2017.10.023

Cell Reports
Article

Genetic Dissection of the Impact of miR-33a and miR-33b during the Progression of Atherosclerosis

Nathan L. Price,[1,2] Noemi Rotllan,[1,2] Alberto Canfrán-Duque,[1,2] Xinbo Zhang,[1,2] Paramita Pati,[1,2] Noemi Arias,[4] Jack Moen,[1,2] Manuel Mayr,[3] David A. Ford,[4] Ángel Baldán,[4] Yajaira Suárez,[1,2] and Carlos Fernández-Hernando[1,2,5,*]
[1]Vascular Biology and Therapeutics Program, Yale University School of Medicine, New Haven, CT 06520, USA
[2]Integrative Cell Signaling and Neurobiology of Metabolism Program, Department of Comparative Medicine, and Department of Pathology, Yale University School of Medicine, New Haven, CT 06520, USA
[3]King's British Heart Foundation Centre, King's College London, London WC2R 2LS, UK
[4]Edward A. Doisy Department of Biochemistry and Molecular Biology and Center for Cardiovascular Research, Saint Louis University School of Medicine, St. Louis, MO 63104, USA
[5]Lead Contact
*Correspondence: carlos.fernandez@yale.edu
https://doi.org/10.1016/j.celrep.2017.10.023

SUMMARY

As an important regulator of macrophage cholesterol efflux and HDL biogenesis, miR-33 is a promising target for treatment of atherosclerosis, and numerous studies demonstrate that inhibition of miR-33 increases HDL levels and reduces plaque burden. However, important questions remain about how miR-33 impacts atherogenesis, including whether this protection is primarily due to direct effects on plaque macrophages or regulation of lipid metabolism in the liver. We demonstrate that miR-33 deficiency in *Ldlr*$^{-/-}$ mice promotes obesity, insulin resistance, and hyperlipidemia but does not impact plaque development. We further assess how loss of miR-33 or addition of miR-33b in macrophages and other hematopoietic cells impact atherogenesis. Macrophage-specific loss of miR-33 decreases lipid accumulation and inflammation under hyperlipidemic conditions, leading to reduced plaque burden. Therefore, the pro-atherogenic effects observed in miR-33-deficient mice are likely counterbalanced by protective effects in macrophages, which may be the primary mechanism through which anti-miR-33 therapies reduce atherosclerosis.

INTRODUCTION

MicroRNAs (miRNAs) have been demonstrated to play a key role in the control of mRNA translation and degradation, constituting an entirely new level of posttranscriptional regulation that is involved in nearly all biological processes (Ambros, 2004; Bartel, 2009; Fernández-Hernando et al., 2011, 2013). Targeting miRNAs is a promising therapeutic approach, as they are dysregulated during and involved in the development of many different disease states (Barwari et al., 2016; Poller et al., 2017). Recent work has elucidated the role of miRNAs in the development of numerous metabolic conditions, including obesity, type II diabetes, and cardiovascular disease, which are responsible for the majority of chronic illnesses and deaths in the United States and other developed countries. Many factors, including insulin signaling, inflammation, autophagy, mitochondrial function, and lipid metabolism, are involved in the development of these cardiometabolic diseases, and previous work suggests a role for miR-33 in regulating all of these critical processes (Allen et al., 2012; Dávalos et al., 2011; Goedeke et al., 2013; Karunakaran et al., 2015; Marquart et al., 2010; Ouimet et al., 2015, 2017; Rayner et al., 2010).

The miR-33 miRNA family, which consists of miR-33a and miR-33b, is one of the most well-characterized examples of miRNA-mediated regulation of lipid metabolism (Marquart et al., 2010; Najafi-Shoushtari et al., 2010; Rayner et al., 2010). *miR-33a* and *miR-33b* are intronic miRNAs encoded within the *SREBP-2* and *SREBP-1* genes, respectively (Marquart et al., 2010; Najafi-Shoushtari et al., 2010; Rayner et al., 2010). Sterol response element binding protein (SREBP)-1 and SREBP-2 are two of the most important transcription factors involved in the regulation of fatty acid and cholesterol metabolism, respectively (Horton et al., 2002). As such, the discovery of miRNAs within intronic regions of the genes that encode these key transcription factors directed multiple groups to investigate whether miR-33a and miR-33b may also be involved in the regulation of lipid metabolism. This work led to the demonstration that miR-33a and miR-33b are co-transcribed along with *SREBP-2* and *SREBP-1* and work in concert with their host genes to help maintain proper lipid levels within the cell (Dávalos et al., 2011; Marquart et al., 2010; Najafi-Shoushtari et al., 2010; Rayner et al., 2010). While the SREBP transcription factors prevent deleterious reductions in cellular lipid levels by promoting lipid synthesis and uptake, miR-33a and miR-33b help prevent further loss of lipids by targeting genes involved in cholesterol trafficking and efflux (Niemann Pick C [NPC1], ATP-Binding Casette A1 [ABCA1], and ATP-Binding Casette G1 [ABCG1]) (Marquart et al., 2010; Najafi-Shoushtari et al., 2010; Rayner et al., 2010) and fatty acid β-oxidation (carnitine palmitoyltransferase 1A [CPT1A], carnitine O-octanoyltransferase [CROT], and hydroxyacyl-coenzyme A [CoA] dehydrogenase/3-ketoacy-CoA thiolase/enoyl-CoA hydratase β subunit

[HADHB]) (Dávalos et al., 2011; Gerin et al., 2010). In addition to regulating cellular cholesterol efflux, ABCA1 also controls the biogenesis of high-density lipoproteins (HDLs) and a number of groups have demonstrated that in vivo antagonism or genetic deletion of miR-33 enhances hepatic ABCA1 expression and increases circulating HDL-cholesterol (HDL-C) (Marquart et al., 2010; Najafi-Shoushtari et al., 2010; Rayner et al., 2010). Further work has demonstrated an additional mechanism by which the miR-33 family prevents lipid depletion in the liver by targeting genes regulating bile acid synthesis and secretion (ATP-binding cassette subfamily B member 11 [ABCB11], amino phospholipid transporter class I type 8B member 1 [ATP8B1], and cytochrome P450 family 7, subfamily A, polypeptide 1 [CYP7A1]) (Allen et al., 2012; Li et al., 2013). Together, these studies established that miR-33 is an important regulator of many facets of lipid metabolism, including several steps of the reverse cholesterol transport (RCT) pathway, the process by which cholesterol is returned to the liver for conversion into bile acids and removal via the feces (Lewis and Rader, 2005; Rader and Hovingh, 2014).

RCT is the only mechanism by which arterial macrophages (Mθs) can remove excess cholesterol, thereby reducing the formation of atherosclerotic plaques by limiting the accumulation of lipid-laden Mθs within the arterial wall (Rosenson et al., 2012). As such, miR-33 has been demonstrated to be an important factor in controlling the development of atherosclerosis, and a great deal of work has been done exploring the possible therapeutic value of inhibiting miR-33 during atherogenesis. Numerous reports have demonstrated that antagonism of miR-33 in mouse models of atherosclerosis can reduce plaque burden by either impeding the progression or promoting the regression of atherosclerotic plaques (Rayner et al., 2011b; Rotllan et al., 2013). However, other similar studies did not observe any beneficial effects of anti-miR-33 therapy on atherogenesis (Marquart et al., 2013). Additionally, some studies of long-term anti-miR-33 treatment have reported deleterious effects, including increased circulating levels of triglycerides (TAGs) and the development of hepatic steatosis (Allen et al., 2014; Goedeke et al., 2014). Most of the beneficial effects of miR-33 on atherosclerosis have been attributed to its ability to increase circulating levels of HDL-C and/or promote Mθ cholesterol efflux (Rayner et al., 2010, 2011b), although additional functions of miR-33, including regulation of mitochondrial function, autophagy, and Mθ activation status, may also contribute to these effects (Karunakaran et al., 2015; Ouimet et al., 2015, 2017). Importantly, studies performed in monkeys have demonstrated that antagonism of miR-33 can also increase circulating levels of HDL-C in non-human primates (Rayner et al., 2011a; Rottiers et al., 2013). These findings are especially relevant, as the intronic region of the *SREBP-1* gene encoding *miR-33b* is disrupted in rodents and other small mammals. Because of the inability to study miR-33b using most conventional animal models, many questions still remain about its specific role in regulation of atherosclerosis and other metabolic disease.

In order to properly assess the possible therapeutic value of anti-miR-33 therapies, it will be necessary to determine whether increased HDL biogenesis or improved cholesterol efflux from plaque Mθs is primarily responsible for mediating the beneficial effects that have been reported. This question is especially relevant, as recent clinical trials have demonstrated that other therapeutic approaches, though effective at raising circulating HDL-C levels, did not appear to have any impact on clinical outcomes in patients with cardiovascular disease. To begin to address this question, Horie and colleagues created mice deficient in miR-33 (Horie et al., 2010). By crossing these animals into the *Apoe*$^{-/-}$ mouse model of atherosclerosis, they were able to demonstrate that whole-body loss of miR-33 reduces atherosclerotic plaque size and lipid content (Horie et al., 2012). Additionally, bone marrow transplant from miR-33-deficient animals into *Apoe*$^{-/-}$ mice, to selectively remove miR-33 from Mθs and other hematopoietic cells, was found to reduce lipid content in atherosclerotic plaques but did not have a significant impact on plaque size (Horie et al., 2012). This study suggests that both increased circulating HDL-C levels and improved efflux of cholesterol from arterial Mθs may contribute to the ability of anti-miR-33 therapies to reduced atherosclerotic plaque burden.

While this work provides some insight into the potential impact of whole-body- versus Mθ-specific antagonism of miR-33, the potential relevance of these findings is limited by the nature of the atherosclerotic mouse model that was used. Because both HDL-C levels and RCT are dramatically reduced in *Apoe*$^{-/-}$ mice, the elevated HDL-C levels seen in mice lacking miR-33 may be substantially more impactful. At the same time, work done using this model may underestimate the impact of miR-33 on regulating Mθ cholesterol efflux, as ABCA1 and ABCG1, two of the most well established targets of miR-33, are primarily responsible for transport of cholesterol onto circulating HDL particles. Additionally, a later report by this same group has demonstrated that loss of miR-33 results in a predisposition to the development of obesity and insulin resistance (Horie et al., 2013), but the impact of these effects on atherosclerosis is unclear, as these phenotypes were not reported in their earlier work in the *Apoe*$^{-/-}$ background.

In this work, we attempt to address many of the outstanding questions regarding how miR-33 regulates atherosclerotic plaque development. To do this, we have generated a novel miR-33 knockout mouse model (*miR-33*$^{-/-}$) and utilized these mice to assess how loss of miR-33 impacts atherosclerosis in the *Ldlr*$^{-/-}$ mouse model of atherosclerosis, in which HDL-C levels and RCT capacity are similar to those in wild-type (WT) mice. Using this model, we are able to demonstrate that miR-33 deficiency results in elevated expression of ABCA1 in both the liver and Mθs and enhances the capacity of Mθs to efflux cholesterol in vivo, leading to a dramatic reduction in the accumulation of cholesterol esters in *miR-33*$^{-/-}$ Mθs under hyperlipidemic conditions. Consistent with this, we observe that selective loss of miR-33 in Mθs and other hematopoietic cells results in a substantial reduction in both atherosclerotic plaque size and lipid content. We further demonstrate that both the number of apoptotic cells and the size of the necrotic cores are reduced in plaques from mice transplanted with *miR-33*$^{-/-}$ bone marrow, indicative of increased plaque stability. Alternatively, whole-body loss of miR-33 in *Ldlr*$^{-/-}$ mice was found to result in increased body weight (BW), impaired insulin sensitivity, and a pro-atherogenic lipid profile. These effects appear to have offset the beneficial effects of miR-33 within the atherosclerotic plaques, as no difference was found in the plaque size or lipid

accumulation of *Ldlr*$^{-/-}$*miR-33*$^{-/-}$ double-knockout (DKO) mice, compared to *Ldlr*$^{-/-}$ controls. We further assess how miR-33b in Mθs impacts atherosclerotic plaque formation using a newly generated mouse model in which the mouse *Srebp-1* gene has been replaced with the human form, including the intronic region encoding miR-33b (*miR-33b*^{KI}). Finally, we have performed in-depth RNA sequencing under both normal and hyperlipidemic (*Ldlr*$^{-/-}$) conditions to provide a more complete view of the impact that ablation of miR-33 has on Mθ gene expression. Together, these findings help clarify the role of miR-33 in the development of atherosclerosis and highlight both the beneficial effects of removing miR-33 in arterial Mθs to promote cholesterol efflux from within atherosclerotic plaques and the deleterious effects that loss of miR-33 in other tissues may have on atherogenesis and other metabolic conditions.

RESULTS

Generation of miR-33 Knockout Mice

To address some of the primary unresolved questions surrounding how miR-33 regulates atherosclerosis, we utilized CRISPR/Cas9 technology to excise the intronic region of the *Srebp-2* gene encoding miR-33, thus generating a new miR-33 knockout mouse model (*miR-33*$^{-/-}$). This excision of roughly 200 bp can be readily confirmed by PCR analysis and has been used to detect effective excision of the miR-33 sequence in all tissues examined (Figure 1A). Consistent with previous studies, western blot analysis of the liver of *miR-33*$^{-/-}$ mice reveals increased expression of miR-33 target genes ABCA1 and HADHβ, compared to control animals, while other miR-33 targets, including CROT, were unaffected (Figure 1B). Consistent with the observed increase in ABCA1 expression, plasma HDL-C levels were found to be elevated in *miR-33*$^{-/-}$ mice as visualized by fast protein liquid chromatography (FPLC) fractionation (Figure 1C) and confirmed by quantification of circulating HDL-C levels (Figure 1D).

Ldlr$^{-/-}$*miR-33*$^{-/-}$ Mice Have Increased BW and Impaired Insulin Sensitivity

Following initial characterization, *miR-33*$^{-/-}$ mice were bred into the low-density lipoprotein receptor (LDLR)-deficient model of mouse atherosclerosis (*Ldlr*$^{-/-}$) to generate *Ldlr*$^{-/-}$*miR-33*$^{-/-}$ (DKO) mice. Similar to earlier work on miR-33-deficient mice fed a high-fat diet (HFD), our DKO mice had significantly higher BW compared to *Ldlr*$^{-/-}$ controls, which was exacerbated by feeding a pro-atherogenic western diet (WD; 1.25% cholesterol) (Figure 1E). Additionally, following 10 weeks of WD feeding, DKO animals showed reduced responsiveness to insulin during an insulin tolerance test (Figure 1F), indicating impaired insulin sensitivity. However, this was not sufficient to disrupt regulation of glucose homeostasis, as neither glucose tolerance tests (Figure 1G) nor measurement of fed and fasted blood glucose levels (Figure 1H) revealed any difference between *Ldlr*$^{-/-}$ and DKO mice at this time. DKO mice also had higher levels of circulating insulin, suggesting that increased insulin production was able to compensate for the impaired insulin sensitivity (Figure 1I). FPLC fractionation of plasma from *Ldlr*$^{-/-}$ and DKO mice following 12 weeks of WD feeding showed that DKO mice had a substantial increase in the amount of cholesterol (Figure 1J) and triglycerides (TAGs) (Figure 1K) in fractions containing very-low-density lipoprotein (VLDL) and low-density lipoprotein (LDL) particles. Furthermore, western blot analysis on FPLC fractions from DKO mice further demonstrates increased expression of the apolipoproteins associated with these particles (Figure 1L). Finally, DKO mice also had elevated total levels of TAGs and cholesterol compared to *Ldlr*$^{-/-}$ controls, while HDL-C levels were not altered (Figures 1M–1O). The similar HDL-C levels observed between *Ldlr*$^{-/-}$ and DKO mice may be due to the repression of *SREBP-2* and miR-33 under hyperlipidemic conditions (Rotllan et al., 2013).

Loss of miR-33 in *Ldlr*$^{-/-}$ Mice Does Not Impact Plaque Size or Morphology

Despite the increased BW, insulin resistance (IR), and pro-atherogenic lipid profile observed in DKO mice, histological analysis of progressive sections of the aortic root did not reveal any major differences between DKO mice and *Ldlr*$^{-/-}$ controls. No significant changes were observed in total plaque area or lipid accumulation, as indicated by oil red O (ORO) staining for neutral lipids (Figure 2A). Similarly, en face analysis of lipid accumulation in the aorta did not show any differences between DKO and *Ldlr*$^{-/-}$ mice (Figure 2B), and measurements of circulating blood leukocytes by fluorescence-activated cell sorting (FACS) and HEMAVET did not reveal any significant differences between groups (Figures S1A and S1B). These findings are contrary to what has been previously observed in most studies in animals treated with anti-miR-33 therapies as well as miR-33-deficient *Apoe*$^{-/-}$ mice. While further work is needed to fully understand the mechanisms underlying the detrimental whole-body changes observed in DKO mice, these findings could suggest that the beneficial effects of removing miR-33 within arterial Mθs may offset these negative effects.

Hematopoietic-Specific Loss of miR-33 Impedes the Development of Atherosclerotic Plaques

To directly address the question of how loss of miR-33 within the Mθs making up atherosclerotic plaques impacts atherogenesis, we performed bone marrow transplants (BMTs) into lethally irradiated *Ldlr*$^{-/-}$ mice using bone marrow (BM) from either WT or *miR-33*$^{-/-}$ mice. Unlike comparisons between *Ldlr*$^{-/-}$ and DKO mice, animals transplanted with BM from *miR-33*$^{-/-}$ mice did not have any differences in plasma lipids or lipoprotein profile (Figures S1C–S1F) and also did not show significant changes in levels of circulating leukocytes (Figures S2A and S2B). However, following 12 weeks of WD feeding, atherosclerotic plaque burden was substantially reduced in mice transplanted with BM from *miR-33*$^{-/-}$ animals. Histological analysis of the aortic root revealed a significant reduction in both total plaque area and lipid accumulation (Figure 3A), and further analysis of en face preps of the aorta also demonstrated a significant decrease in lipid accumulation (Figure 3B). More detailed analysis of these plaques showed that the size of the necrotic core was also decreased in mice transplanted with miR-33$^{-/-}$ BM (Figure 3C). The percentage of plaque area that stained positive for the Mθ marker CD68 was similar to that of control animals, indicating that the proportion of the plaque made up of macrophages

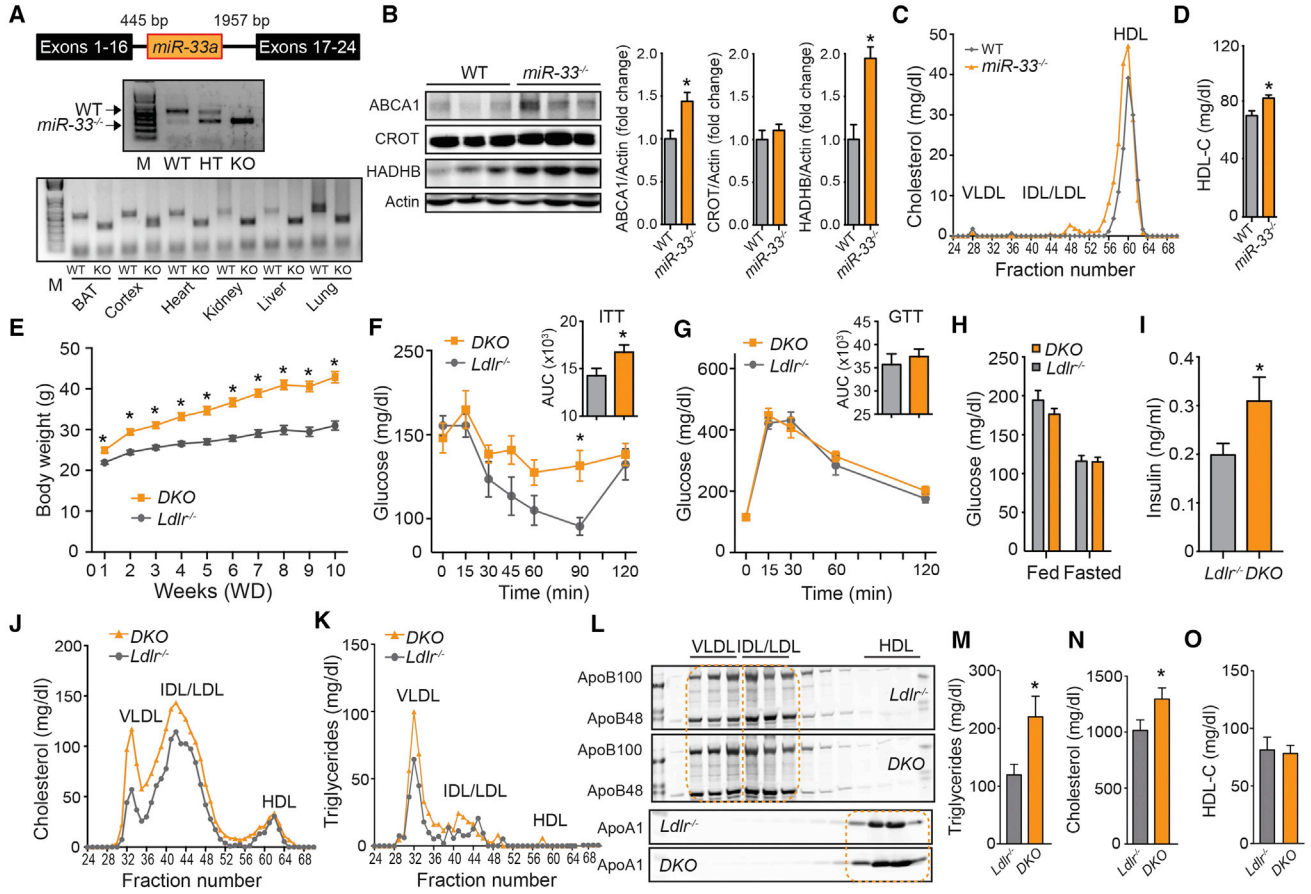

Figure 1. Global Deletion of miR-33 in *Ldlr*$^{-/-}$ Mice Results in Obesity, IR, and Dyslipidemia

(A) Strategy used to generate *miR-33*$^{-/-}$ mice (upper panel). PCR analysis of tail DNA isolated from WT, *miR-33*$^{+/-}$, and *miR-33*$^{-/-}$ mice (middle panel). PCR analysis showing the deletion of miR-33 in the indicated tissues (bottom panel).

(B) Representative western blot analysis of ABCA1, CROT, and HADHB in liver samples isolated from WT and *miR-33*$^{-/-}$ mice. Relative protein levels were determined by band densitometry and are expressed in a.u. after correction for loading control actin (n = 3).

(C) Lipoprotein profile analysis from pooled plasma of WT and *miR-33*$^{-/-}$ mice.

(D) Plasma HDL-C levels from WT and *miR-33*$^{-/-}$ mice (n = 9).

(E) BW of *Ldlr*$^{-/-}$ and *Ldlr*$^{-/-}$*miR-33*$^{-/-}$ (DKO) mice fed a western diet (WD) for 10 weeks (n = 9).

(F and G) Insulin tolerance test (ITT) (F) and glucose tolerance test (GTT) (G) in *Ldlr*$^{-/-}$ and DKO mice fed a WD for 10 weeks (n = 6–7). Inset represents the area under the curve (AUC).

(H) Plasma glucose levels in fed and fasted 2-month-old *Ldlr*$^{-/-}$ and DKO mice (n = 7).

(I) Plasma insulin levels in fasted *Ldlr*$^{-/-}$ and DKO mice fed a WD for 12 weeks.

(J and K) Cholesterol (J) and TAG content (K) of FPLC-fractionated lipoproteins from pooled plasma of *Ldlr*$^{-/-}$ and DKO mice fed a WD for 12 weeks.

(L) Western blot analysis (representative of two blots) of plasma APOB and APOA1 in the FPLC-fractionated lipoproteins in panel. Lanes 1–13 correspond to the following pooled fractions: 1 (28–30), 2 (31–33), 3 (34–36), 4 (37–39), 5 (40–42), 6 (43–45), 7 (46–48), 8 (49–51), 9 (52–54), 10 (55–57), 11 (58–60), 12 (61–63), and 13 (64–66).

(M–O) Plasma TAGs (M), total cholesterol (N), and HDL-C (O) in the plasma of *Ldlr*$^{-/-}$ and DKO mice fed a WD for 12 weeks (n = 11–16).

All data represent mean ± SEM. *p < 0.05, comparing *miR-33*$^{-/-}$ with WT mice or DKO with LDLR$^{-/-}$ mice on the same diet.

was not impacted by loss of miR-33. Alternatively, CD68/TUNEL co-staining was decreased in plaques from animals that received *miR-33*$^{-/-}$ BM, indicating that Mθ apoptosis may contribute to the elevated formation of necrotic cores in WT animals (Figure 3D). Furthermore, by digesting the aortas of WD-fed mice and performing FACS analysis, we were able to show a significant decrease in the number of both total and activated (Ly-6C^{high}) Mθs in plaques from mice transplanted with *miR-33*$^{-/-}$ BM (Figure 3E). Together, these findings demonstrate that, while hematopoietic loss of miR-33 does not alter the proportion of the plaque that is made up of macrophages, there is an overall decrease in the number of macrophages within the arterial wall corresponding to the overall decrease in plaque size.

Generation of miR-33b Knockin Mice

While these findings highlight the important role of Mθ miR-33 in the regulation of atherogenesis in mice, the situation is more complicated in humans due to the presence of a second

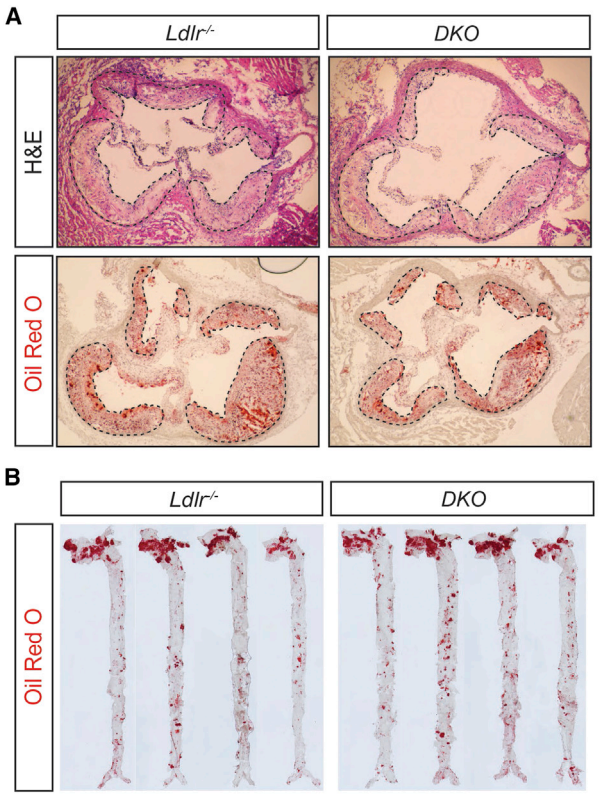

Figure 2. Germline Deficiency of miR-33 Does Not Influence the Progression of Atherosclerosis

(A) Representative histological analysis of cross-sections of the aortic sinus stained with H&E (upper panels) or oil red O (ORO; bottom panels) of $Ldlr^{-/-}$ and $Ldlr^{-/-}miR\text{-}33^{-/-}$ (DKO) mice fed a western diet (WD) for 12 weeks. Right panels: the mean lesion area and neutral lipid accumulation calculated from H&E and ORO aortic cross-sections, respectively. Each dot represents the mean of the quantification of ≥9 sections from an individual animal (n = 10–11 animals per group).

(B) Representative en face ORO staining of 4 aortas from $Ldlr^{-/-}$ and DKO mice fed a WD for 12 weeks. Quantification of the ORO-positive area is shown in the right panel and represents the mean ± SEM (n = 10).

All data represent mean ± SEM. *p < 0.05, comparing DKO with $Ldlr^{-/-}$ mice on the same diet. NS, not significant.

miR-33 isoform, miR-33b. To determine whether miR-33b may also impact atherosclerosis, we generated a novel mouse model in which the entire mouse *Srebp-1* gene has been replaced with the human sequence, including the region encoding miR-33b, under the control of the mouse promoter ($miR\text{-}33b^{KI}$). Insertion of this construct can be confirmed by the presence of the neo cassette, which was later excised, or with specific primers demonstrating the presence of human *Srebp-1* or the loss of mouse *Srebp-1* (Figure S3A). Furthermore, the introduction of human *SREBP-1* and miR-33b, and the loss of mouse *Srebp-1* in homozygous $miR\text{-}33b^{KI}$ mice, was confirmed by qPCR analysis (Figures S3B, S3C, and S3E). Importantly, this analysis also demonstrates that the expression of *Srebp-2* and miR-33a was not altered by the addition of miR-33b (Figures S3D and S3F). Expression of miR-33b was detected in a variety of tissues, among which the liver showed the highest expression levels (Figure S3G). This is consistent with what has previously been shown for miR-33b in human tissues (Najafi-Shoushtari et al., 2010). Human *SREBP-1* also had high levels of expression in the liver, although it was also highly expressed in other tissues, including the white adipose tissue (WAT) and kidney, which had relatively low levels of miR-33b expression (Figure S3H).

Reconstitution with BM from Cells Expressing miR-33b Does Not Impact Atherosclerotic Plaque Formation

Similar to BMT experiments with $miR\text{-}33^{-/-}$ mice, transplantation of $Ldlr^{-/-}$ mice with BM from $miR\text{-}33b^{KI}$ animals did not have any impact on lipid profiles or circulating blood leukocytes (Figures S4A–S4D). Unlike the loss of miR-33, however, introduction of Mθs expressing miR-33b also did not have any impact on total plaque size or lipid accumulation in either the aortic root or whole aorta (Figure S5A). These findings are likely due to the low levels of expression of miR-33b within Mθs compared to that of miR-33a. While miR-33b can be readily detected in Mθs either from $miR\text{-}33b^{KI}$ mice or derived from human peripheral blood mononuclear cells (PBMCs), its expression in these cells is dramatically lower than that of miR-33a (Figure S5B). Consistent with this, the expression of miR-33 target genes was not changed in Mθs from $miR\text{-}33b^{KI}$ mice either under basal conditions, following stimulation with an LXR ligand (T0901317), or loading with acetylated LDL (Ac-LDL) (Figure S5C). Unfortunately, assessment of how addition of miR-33b across the whole body impacts atherosclerosis was not possible, due to the sub-Mendelian birth rates, poor survival, and reduced size of $miR\text{-}33b^{KI}$ mice.

Loss of miR-33 Improves Mθ RCT In Vivo

Although the metabolic differences observed in $miR\text{-}33^{-/-}$ mice did not impede overall assessment of atherogenesis, the altered BW, IR, and lipid levels of DKO mice preclude any direct examination of how changes in HDL biogenesis contribute to these changes. As such, we next sought to better understand the mechanisms underlying the beneficial effects observed in BMT experiments with miR-33-deficient donors. Previous work has demonstrated that inhibition of miR-33 enhances Mθ cholesterol efflux (Marquart et al., 2010; Najafi-Shoushtari et al., 2010; Rayner et al., 2010). Consistent with this, we found that the expression of ABCA1 and ABCG1 is increased in Mθs isolated from $miR\text{-}33^{-/-}$ mice (Figure 4A). Next, we determined whether the absence of miR-33 in Mθs enhances RCT. To this end, bone-marrow-derived Mθs (BMDMs) from WT or $miR\text{-}33^{-/-}$ mice were differentiated in vitro, pre-loaded with [H^3]-cholesterol, and injected into the peritoneal cavity of WT mice (Figure 4B). By quantifying the amount of [H^3]-cholesterol incorporated into

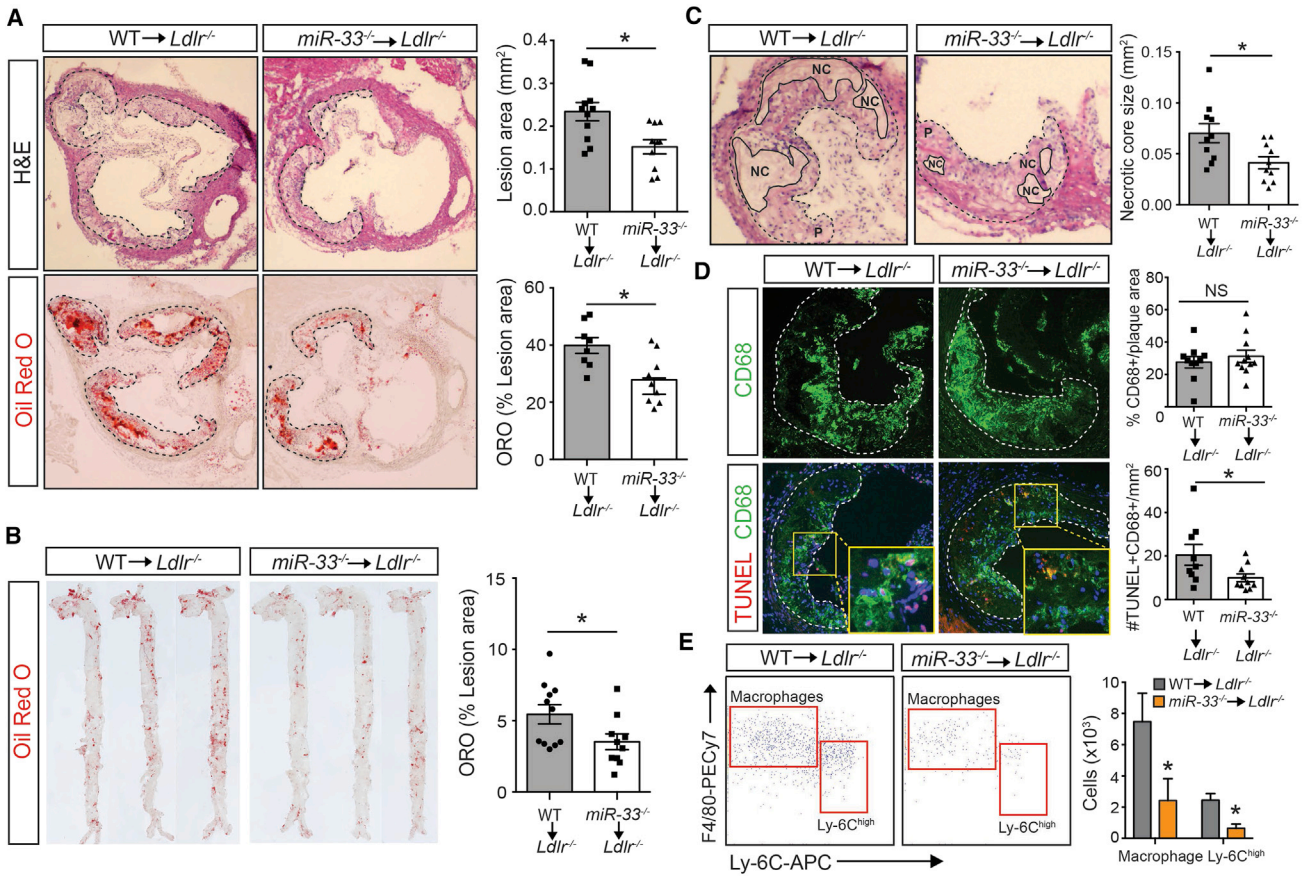

Figure 3. Hematopoietic miR-33 Deficiency Attenuates Atherogenesis

(A) Left: representative histological analysis of cross-sections of the aortic sinus stained with H&E (upper panels) or oil red O (ORO; lower panels) of *Ldlr*$^{-/-}$ mice transplanted with WT or *miR-33*$^{-/-}$ bone marrow (BM) fed a western diet (WD) for 12 weeks. Right: the mean lesion area and neutral lipid accumulation calculated from H&E or ORO aortic cross-sections, respectively. Each dot represents the mean of the quantification of ≥9 sections from an individual animal (n = 8–11 animals per group).

(B) Representative en face ORO staining of aortas from *Ldlr*$^{-/-}$ mice transplanted with WT and *miR-33*$^{-/-}$ BM and fed a WD for 12 weeks. Quantification of the ORO-positive area is shown in the right panel and represents the mean ± SEM (n = 10–11 per group).

(C) Representative images of aortic root cross-sections stained with H&E from *Ldlr*$^{-/-}$ mice transplanted with WT or *miR-33*$^{-/-}$ BM fed a WD for 12 weeks. Images reveal how the necrotic core area was defined for quantification in each section. Dashed lines indicate the boundary of the developing necrotic core (NC). Quantification is shown in the right panel. Each dot represents the mean of the quantification of ≥9 sections from an individual animal (n = 10 animals per group).

(D) Representative cross-section analysis of macrophage (Mθ) content (CD68-positive cells; upper panels) and apoptotic cells (TUNEL-positive cells; bottom panels) of the aortic root from *Ldlr*$^{-/-}$ mice transplanted with WT or *miR-33*$^{-/-}$ BM and fed a WD for 12 weeks. Quantifications are the graphs on the right. Each dot represents the mean of the quantification of ≥9 sections from an individual animal (n = 9–11 animals per group).

(E) Flow cytometry analysis of aortic Mθs and monocytes from *Ldlr*$^{-/-}$ mice transplanted with WT or *miR-33*$^{-/-}$ BM and fed a WD for 12 weeks. Left: representative dot plots showing gating schemes. Right: quantification of total number of Mθs or Ly-6C^{high} monocytes per aorta (n = 6).

All data represent mean ± SEM. *p < 0.05, comparing *Ldlr*$^{-/-}$ mice transplanted with *miR-33*$^{-/-}$ BM to *Ldlr*$^{-/-}$ mice transplanted with WT BM on the same diet.

the blood and feces of these animals over 48 hr, we were able to demonstrate that loss of miR-33 improves RCT from Mθs in vivo, resulting in a significant increase in radioactivity counts in both the plasma and feces (Figure 4C). These results represent the first demonstration that loss of miR-33 in Mθs accelerates RCT in vivo.

Mθs Lacking miR-33 Have Reduced Levels of Cholesterol Esters and Phospholipids

To determine how this increased RCT capacity impacts the lipid content of *miR-33*$^{-/-}$ Mθs, we performed lipidomic analysis of thioglycollate-elicited peritoneal Mθs from WT, *miR-33*$^{-/-}$, *LDLR*$^{-/-}$, and *DKO* mice under normal (WT) or hypercholesterolemic (*Ldlr*$^{-/-}$) conditions (Figure 4D). Consistent with our previous results, we observe a significant decrease in the accumulation of cholesterol esters (CEs) in miR-33-deficient Mθs from *Ldlr*$^{-/-}$ mice (Figure 4E), including reductions in all CE subspecies (Figure 4F). Interestingly, in a WT background, loss of miR-33 was also found to significantly reduce the amount of Mθ phosphatidylethanolamines (PEs) and phosphatidylserines (PSs) (Figures 4E and 4G). These lipid subspecies are important

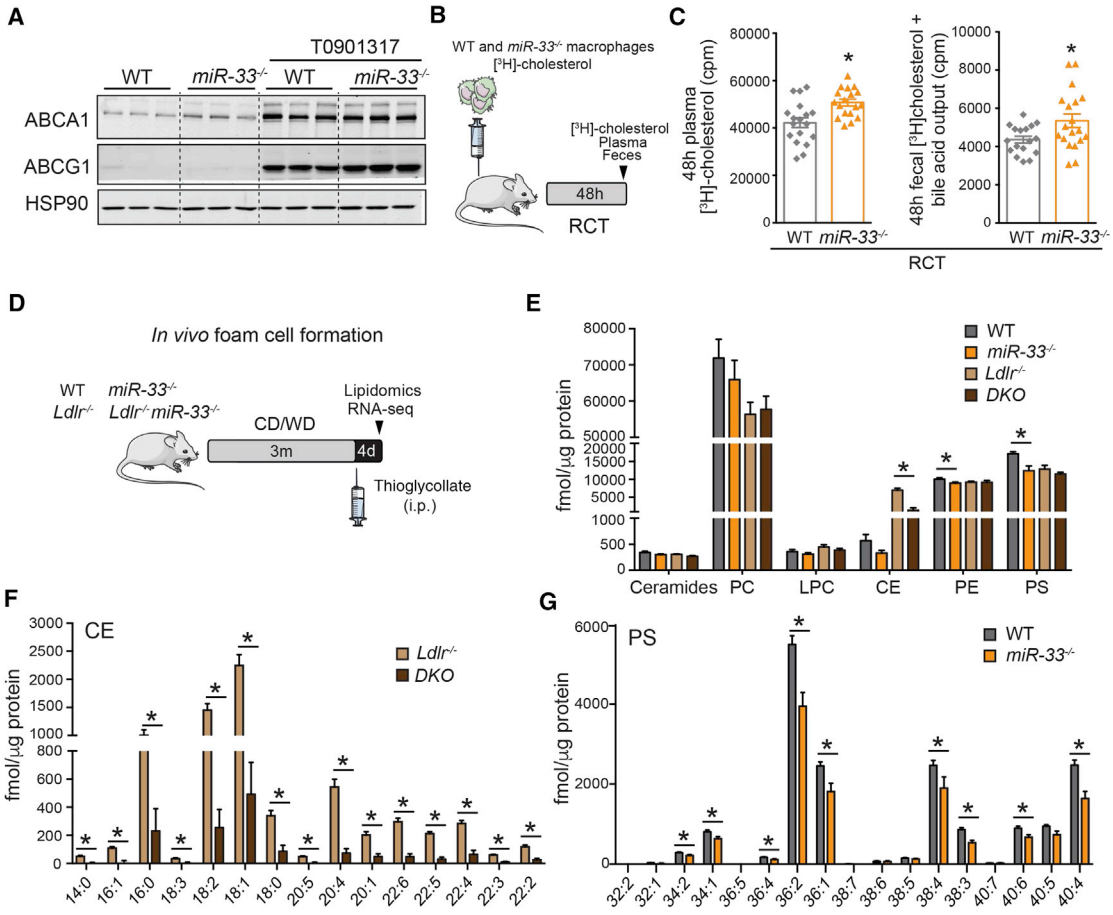

Figure 4. Absence of miR-33 in Macrophages Increases ABCA1 Expression, Enhances RCT, and Attenuates Lipid Accumulation In Vivo

(A) Representative western blot analysis of ABCA1 and ABCG1 expression in peritoneal macrophages (Mθs) isolated from WT and *miR-33*$^{-/-}$ mice untreated and treated with T0901317. HSP90 is used as a loading control.

(B) Schematic representation of the RCT experiment. WT and *miR-33*$^{-/-}$ bone-marrow-derived Mθs (BMDM) are loaded with [^{3}H]-cholesterol and injected into WT mice. Exit of [^{3}H]-cholesterol from Mθs is measured in the plasma and feces 48 hr after injection.

(C) [^{3}H]-cholesterol in plasma (left panel) and in feces (right panel) from WT mice injected subcutaneously with [^{3}H]-cholesterol-labeled BMDM from WT or *miR-33*$^{-/-}$ mice (n = 18).

(D) Schematic representation of the lipidomic and genomic analyses of Mθ foam cells isolated in vivo from *Ldlr*$^{-/-}$ and *Ldlr*$^{-/-}$*miR-33*$^{-/-}$ (DKO) mice fed a chow diet (CD) or western diet (WD) for 12 weeks.

(E–G) Lipidomic analysis of WT, *miR-33*$^{-/-}$, *Ldlr*$^{-/-}$, and DKO Mθs. (E) Levels of ceramides, phosphatidylcholine (PC), lysophosphatidylcoline (LPC), cholesterol esters (CE), phosphatidylethanolamine (PE), and phosphatidylserine (PS). (F) Levels of CE species. (G) Levels of PS species (n = 4–6).

All data represent mean ± SEM. *p < 0.05, comparing *miR-33*$^{-/-}$ with WT mice or DKO with *Ldlr*$^{-/-}$ mice on the same diet.

components of cellular membranes and are involved in a number of important cellular functions, including apoptosis, migration, and phagocytosis (Greenberg et al., 2006; Mariño and Kroemer, 2013; Shiratsuchi et al., 1998).

Mθs Deficient in miR-33 Do Not Show Differences in In Vitro Polarization or Apoptosis but Do Have Increased Efferocytosis Capacity

To further determine what effects of miR-33 deficiency in Mθs may contribute to the observed differences in plaque formation, we performed a series of experiments to assess Mθ functions related to atherogenesis. Previous reports have suggested that miR-33 can directly regulate Mθ activation status and inflammatory response (Ouimet et al., 2015; Rayner et al., 2011b), and our own data show that the number of Ly-6C^{hi}-activated Mθs (M1-like) is reduced in plaques from mice reconstituted with *miR-33*$^{-/-}$ BM. However, induction of Mθ polarization in vitro did not reveal any significant differences between WT and *miR-33*$^{-/-}$ Mθs (Figures S6A–S6G). Treatment with lipopolysaccharide (LPS)/interferon (IFN)γ stimulates the BMDM toward a classical (M1-like) activation status and induction of a number of inflammatory genes. While the induction of interleukin (IL)-6 and IL-1β is somewhat diminished in Mθs deficient in miR-33, these changes do not reach statistical significance (Figures S6A and S6B). Moreover, loss of miR-33 does not have any impact on the induction of other markers of classically activated

Mθ, NOS2, or COX2, either at the gene expression or the protein level (Figures S6C–S6E). Additionally, following treatment with IL-4, to stimulate an alternative (M2-like) activation status, we did not find any differences in the expression of markers of alternatively activated Mθs, ARG1 and FIZZ1 (Figures S6F and S6G). Together, these findings suggest that the changes in Mθ accumulation and activation within the plaque may not be due to direct regulation of Mθ polarization by miR-33.

Similarly, we did not observe any differences in the induction of apoptosis in miR-33-deficient Mθs in response to cholesterol loading. Treatment of Mθs with Ac-LDL and an ACAT inhibitor (Sandoz) to induce excessive free cholesterol accumulation resulted in apoptosis in approximately 15% of WT cells and was not significantly altered in Mθs lacking miR-33 (Figure S6H). While these in vitro experiments do not properly reflect conditions within the atherosclerotic plaque, they do suggest that factors other than reduced apoptosis may contribute to the lower numbers of TUNEL-positive cells and decreased necrotic core size found in plaques from animals transplanted with miR-33-deficient BM. Consistent with this, we found that loss of miR-33 increases the ability of Mθs to engulf and incorporate fluorescently labeled apoptotic cells (Figure S6I). Interestingly, the expression of MERTK, a kinase involved in the regulation of efferocytosis, was found to be upregulated in *miR-33*$^{-/-}$ Mθs (Figure S6J). These findings are important, as efficient clearance of apoptotic cells limits prolonged inflammation and may contribute to the reduced recruitment and activation of Mθs lacking miR-33.

Lack of miR-33 in Mθs Attenuates the Expression of Genes Associated to Inflammatory Response In Vivo

Similar to our lipidomic analysis, we have also performed an unbiased analysis of how gene expression levels are impacted by loss of miR-33 in Mθs in vivo under hyperlipidemic (*Ldlr*$^{-/-}$) conditions. This approach, developed by the Glass laboratory, allows the analysis of changes in lipid metabolism and gene expression during foam-cell formation in vivo (Li et al., 2004). RNA sequencing (RNA-seq) analysis has revealed a number of pathways and specific genes that may be involved in mediating the effects of miR-33 on Mθ function and atherosclerotic plaque formation. Furthermore, a comparison between WT and *Ldlr*$^{-/-}$ mice allows us to distinguish between those genes that are generally regulated in response to changes in lipid content and those that are more likely to be directly regulated by miR-33 (Figure 5). Among those factors found to be significantly altered in response to loss of miR-33 (Figure 5B), a number of important pathways were found to be overrepresented, including those involved in inflammation, fatty acid metabolism, cholesterol biosynthesis, and unfolded protein response (Figures 5C and 5D). These pathways and many of the genes within them are known to play an important role in the development of atherosclerotic plaques and may contribute either directly or indirectly to the beneficial effects observed in miR-33-deficient Mθs. Additional analysis of gene expression changes between WT and *Ldlr*$^{-/-}$ mice demonstrates that many of these same pathways are also impacted by hypercholesterolemia. Indeed, many of the metabolic pathways that are upregulated in DKO-deficient macrophages compared to *Ldlr*$^{-/-}$ mice are downregulated in *Ldlr*$^{-/-}$ mice compared to WT (Figure 5E). This suggests that these changes may be largely due to differences in lipid content, while pathways related to stress response are downregulated in both comparisons, indicating that these changes are likely regulated by factors independent of lipid content. Indeed, these changes would be predicted to result in diminished inflammatory signaling through the NFκB (nuclear factor κB)- and TLR4-mediated pathways, resulting in a reduction in Mθ activation and polarization in vivo (Figures 6A and S7). Moreover, some of the specific changes in lipid sub-species that we have observed in *miR-33*$^{-/-}$ macrophages may also contribute to the observed changes in inflammatory response. Among the molecules that are known to interact with phosphatidylserine and phosphatidylethanolamine, many were found to be dysregulated by loss of miR-33 in our RNA-seq analysis. Indeed, the observed decreases in these two classes of lipids could be predicted to promote many of these changes in gene expression, and the overall changes in these genes are predicted to result in a decrease in inflammatory response (Figure 6B). While additional work will be needed to identify the specific miR-33 targets responsible for mediating many of these effects, these data provide an important resource for establishing how changes in lipid content and miR-33 levels impact global gene expression patterns in Mθs in vivo.

Overall, this work demonstrates that loss of miR-33 selectively in hematopoietic cells is sufficient to reduce Mθ recruitment and lipid accumulation in atherosclerotic plaques. The beneficial effects, however, are offset by the pro-atherogenic factors that are found to be increased in response to whole-body loss of miR-33, including increased BW, IR, and dyslipidemia. Alternatively, Mθ miR-33b was not found to have a major impact on atherosclerosis, which is likely due to the low expression of this isoform in Mθs compared to miR-33a (Figure 7).

DISCUSSION

As a known regulator of cholesterol efflux and HDL-C metabolism, miR-33 is an attractive target for the treatment of cardiovascular disease, and several studies have found that antagonism of miR-33 can reduce atherosclerotic plaque burden (Karunakaran et al., 2015; Ouimet et al., 2015; Rayner et al., 2011b; Rotllan et al., 2013). Another study did not find reduced aortic lesions in anti-miR-33-treated mice (Marquart et al., 2013). However, the hypertriglyceridemia and hepatic steatosis observed in some long-term anti-miR-33 studies (Allen et al., 2014; Goedeke et al., 2014) and the adverse metabolic effects reported in miR-33 knockout mice (Horie et al., 2013) have raised major concerns about the development of anti-miR-33 therapeutics for treatment of human patients. Much of this concern stems from an incomplete understanding of the mechanisms by which miR-33 impacts atherogenesis, as highlighted by the dual role of miR-33 regulating cholesterol efflux in Mθs and HDL biogenesis in the liver. This question is even more important, due to the poor performance of CETP inhibitors and other HDL-C-raising therapies in recent clinical trials (Rader and deGoma, 2014; Rader and Hovingh, 2014). If the effects of miR-33 are primarily due to its ability to raise circulating HDL-C levels, anti-miR-33 therapeutics may face many of the same issues found in these

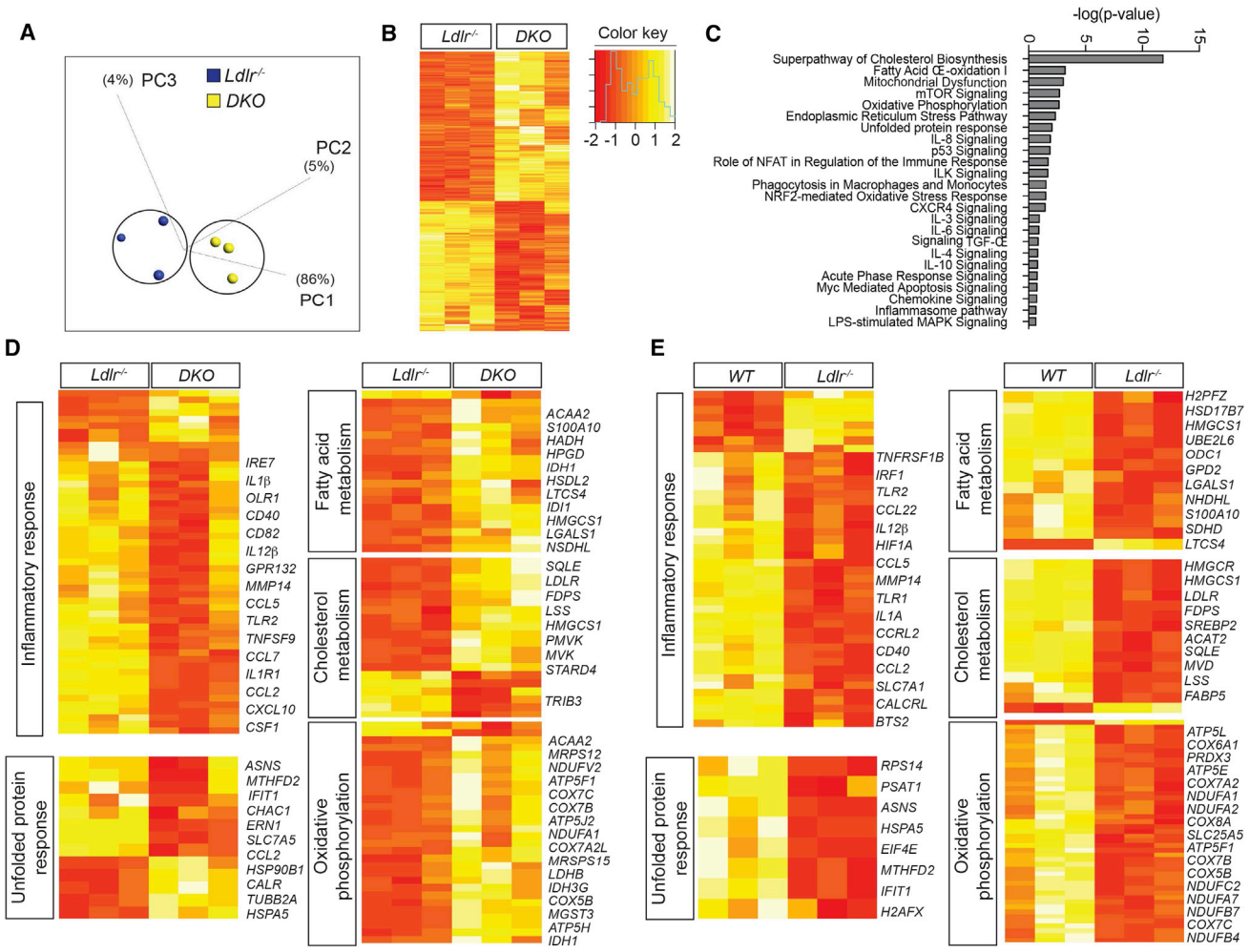

Figure 5. Lack of miR-33 in Macrophages Impacts Genes Involved in Stress Response and Metabolic Function In Vivo

(A) Principal-component (PC) analysis of peritoneal macrophages (Mθs) from *Ldlr*$^{-/-}$ and *Ldlr*$^{-/-}$*miR-33*$^{-/-}$ (DKO) mice (n = 3) based on RNA-sequencing gene expression levels, color coded according to the group of mice.

(B) Heatmaps representing gene expression (rlog-transformed values) of genes differentially expressed between *Ldlr*$^{-/-}$ and DKO Mθs.

(C) Top canonical pathways involving differentially expressed molecules and related to atherosclerosis expressed as −log (p value).

(D) Heatmaps of pathways relevant to atherosclerosis that are altered in DKO mice compared to *Ldlr*$^{-/-}$ controls.

(E) Heatmaps of pathways relevant to atherosclerosis that are altered in *Ldlr*$^{-/-}$ mice compared to WT controls.

studies, while direct effects on the ability of arterial Mθs to efflux cholesterol may provide greater therapeutic value. Together, the findings laid forth in this article help clarify many of the questions regarding how miR-33 regulates atherosclerotic plaque formation, which will be necessary for evaluating the possible therapeutic potential of miR-33 antagonists.

Similar to previous work in *Apoe*$^{-/-}$ mice (Horie et al., 2012), we observe that reconstitution of *Ldlr*$^{-/-}$ mice with BM deficient in miR-33 reduces lipid accumulation in atherosclerotic plaques. However, the effects observed in our study are considerably more robust, with significant reductions also observed in total plaque size, necrotic core area, and the number of apoptotic cells. Since the primary function of ABCA1 and ABCG1 is the efflux of cholesterol onto poorly lipidated ApoA1 and HDL particles, respectively (Tall et al., 2008), these differences may be due to the low levels of HDL-C in *Apoe*$^{-/-}$ mice, which could limit the impact of elevating Mθ ABCA1 levels. These findings indicate that the ability of miR-33 to promote cholesterol efflux from arterial Mθs plays a more important role in its regulation of atherosclerosis than was suggested by previous work. Because these effects are independent of any changes in circulating HDL-C levels, these findings demonstrate the potential therapeutic value of anti-miR-33 therapies for promoting the removal of lipids from atherosclerotic plaques and, thereby, limiting plaque development.

Interestingly, we find that loss of miR-33 in *Ldlr*$^{-/-}$ mice results in a significant increase in BW, which is exacerbated by a WD feeding. This predisposition to diet-induced obesity is also accompanied by decreased insulin sensitivity and increased circulating levels of VLDL-C, and LDL-C and TAGs. Together,

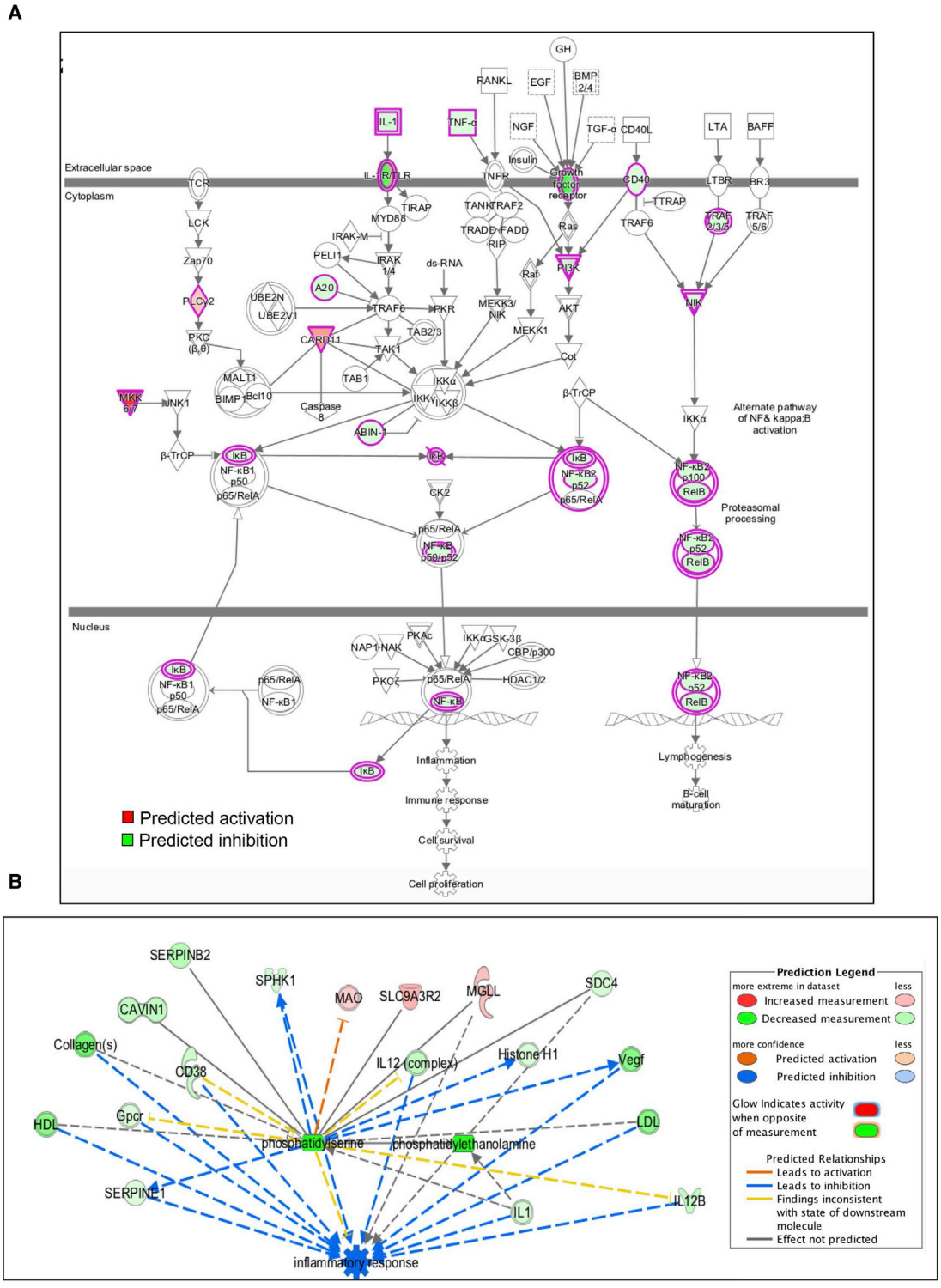

Figure 6. Absence of miR-33 Attenuates NFKB Activation and Innate Immune Response

(A) NFKB signaling pathway analysis using the Ingenuity Pathway Analysis (IPA) tool. Genes represented in green are downregulated in peritoneal macrophages (Mθs) isolated from *Ldlr*$^{-/-}$*miR-33*$^{-/-}$ (DKO) compared to Mθs obtained from *Ldlr*$^{-/-}$ mice.

(B) Network of genes known to interact with phosphatidylserine and phosphatidylethanolamine whose expression is significantly altered in miR-33-deficient macrophages. Prediction analysis identifies genes in which inhibition (blue) or activation (red) is predicted based on changes in these lipid species. Overall changes in this network are predicted to inhibit inflammatory response.

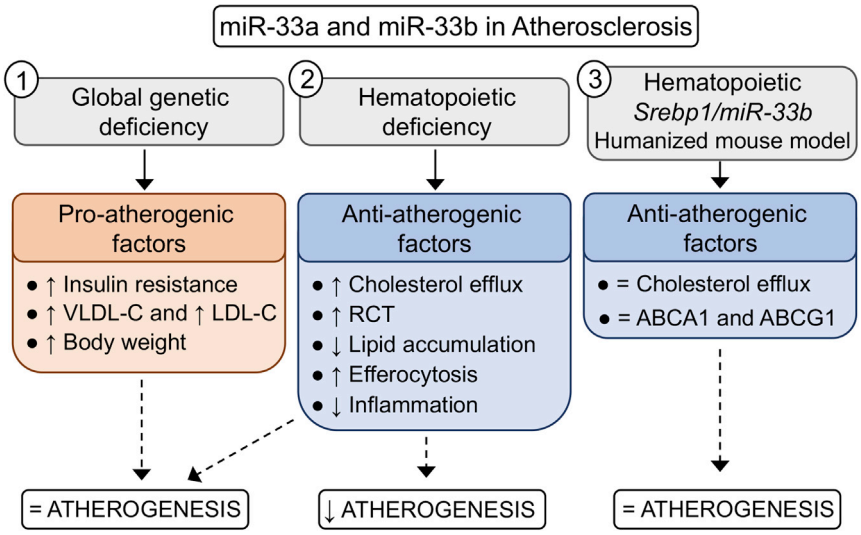

Figure 7. Schematic Representation of the Role of miR-33a and miR-33b in Atherogenesis

these changes likely offset the beneficial effects occurring in plaque Mθs, as there were no differences in plaque size or lipid accumulation in *Ldlr*$^{-/-}$ mice lacking miR-33. Unfortunately, these changes also impede our ability to address the specific impact of miR-33's regulation of HDL biogenesis and bile acid metabolism in the liver. While BMT from WT mice into *Ldlr*$^{-/-}$ and DKO animals would allow us to determine how effects on the liver and other tissues impact plaque formation, it would not help with dissociating the effects on RCT from the changes observed in BW, IR, and circulating lipids. These effects are contrary to what was previously reported in *Apoe*$^{-/-}$ mice lacking miR-33, where the authors did find reduced plaque size; did not observe any difference in circulating VLDL-C, LDL-C, or TAGs; and did not provide any data on BW or insulin sensitivity (Horie et al., 2012). Interestingly, a later report by the same group did show a dramatic increase in BW and IR in *miR-33*$^{-/-}$ mice when fed a high-fat (60% saturated fat) diet (Horie et al., 2013). Further work is currently underway seeking to elucidate the specific mechanisms by which miR-33 regulates obesity and IR, as this will be important for the progress of any anti-miR-33 therapeutic efforts.

While most work on miR-33 has been done using mouse models, humans contain a second miR-33 isoform, miR-33b, which may also play an important role in atherosclerosis. In this work, we begin to assess the impact of miR-33 on atherogenesis by performing BM transplants from *miR-33b*^{KI} mice into the *Ldlr*$^{-/-}$ background. Addition of miR-33b to Mθs does not appear to have any impact on plaque formation or lipid accumulation. These results are likely due to the relatively low expression of miR-33b in Mθs, compared to that of miR-33a. This finding is not specific to our *miR-33b*^{KI} mice, as Mθs derived from human peripheral blood mononuclear cells also expressed much higher levels of miR-33a compared to miR-33b. These differences in miRNA expression vary between cell types, suggesting that the role of miR-33b in the liver, where miR-33b is most highly expressed both in our mouse model and in human tissues (Najafi-Shoushtari et al., 2010), and other tissues may be considerably more important. Consistent with this, a previously described miR-33b knockin model was reported to have decreased expression of ABCA1 and other miR-33 target genes in primary hepatocytes (Horie et al., 2014). Furthermore, we found that expression of miR-33b in the liver is higher than that of miR-33a, which could be very interesting under conditions of obesity and IR, where the host gene of miR-33b, *SREBP-1*, is known to be dysregulated. Unfortunately, the poor survival rates and reduced BW of homozygous *miR-33b*^{KI} mice at birth and throughout early adulthood has precluded any meaningful exploration into how global addition of miR-33b impacts atherogenesis. Further work using adult inducible models or other techniques to overcome these developmental issues will be needed to properly address the role of miR-33b in atherosclerosis and other metabolic diseases.

A number of different functions of miR-33 have been described as possibly contributing to its regulation of atherosclerotic plaque formation. Among these, the ability of miR-33 to regulate Mθ cholesterol efflux and RCT is the most likely to directly impact the accumulation of lipids within arterial Mθs (Rayner et al., 2010, 2011b). In this work, we demonstrate for the first time that loss of miR-33 increases the capacity of Mθs to efflux cholesterol in vivo. Additionally, we observed an additional function of miR-33 in regulating the uptake of apoptotic cells by Mθs in vitro, which could possibly also contribute to the changes seen in necrotic core size. Interestingly, another group has very recently reported similar changes in efferocytosis upon inhibition of miR-33, which were attributed to the regulation of autophagy by miR-33 (Ouimet et al., 2017). However, neither the specific autophagic genes reported to be targeted by miR-33 nor most other genes related to autophagic function were found to be significantly altered in our RNA-seq analysis. Alternatively, MERTK protein levels were found to be reduced in miR-33-deficient Mθs, and miRNA prediction algorithms suggest that this may targeted by the passenger strand of miR-33, miR-33*. Finally, by using unbiased techniques for assessing global changes in lipid profiles, and mRNA expression, we provide a comprehensive profile of the factors influenced by miR-33 under normal and hyperlipidemic conditions, which provides further insight into the pathways and individual gene targets responsible for mediating the effects of miR-33.

Consistent with the increased capacity to efflux cholesterol previously observed, we find a dramatic reduction in the accumulation of all different species of cholesterol esters in miR-33-deficient Mθs under hyperlipidemic conditions. Our RNA-seq analysis in Mθs has revealed a number of genes that are differentially up- and downregulated in response to loss of miR-33. Pathway analysis further revealed that many of these genes

are involved in pathways that have previously been shown to be important for the development of atherosclerosis. An additional analysis, identifying genes that are altered under hyperlipidemic conditions, demonstrates that many of the genes whose expression was dysregulated in response to hyperlipidemic conditions were regulated in a reverse manner in cells lacking miR-33. These changes are likely due to the reduced lipid accumulation observed in miR-33-deficient Mθs; however, a large proportion of the genes dysregulated in response to loss of miR-33 were not found to be altered in response to dyslipidemia, suggesting that these could be either directly or indirectly regulated by miR-33 independent of its effects on lipid content. Among the pathways found to be significantly overrepresented in this dataset were important pathways involved in regulation of metabolic function. Most of the genes in these pathways were significantly upregulated in DKO animals. These same pathways were largely repressed in *Ldlr*$^{-/-}$ mice compared to WT, suggesting that the reduced lipid accumulation in DKO animals is likely the primary factor responsible for the altered expression of these genes. Alternatively, most of the genes in pathways related to inflammation and endoplasmic reticulum (ER) stress (unfolded protein response) were downregulated both in DKO mice compared to *Ldlr*$^{-/-}$ and *Ldlr*$^{-/-}$ mice compared to WT, despite opposite changes in lipid content. Therefore, the alterations in these stress response pathways is likely independent of the overall changes in lipid content. While these alterations may be mediated through direct targeting of factors involved in regulation of these pathways, our in vitro assessment of Mθ polarization and ER-stress-mediated apoptosis did not reveal any differences between *miR-33*$^{-/-}$ and WT Mθs.

Interestingly, we also found reduced levels of phosphatidylserine and phosphatidylethanolamine in miR-33-deficient Mθs. These changes are not as uniform or dramatic as the reductions in cholesterol esters but may have important effects, as these lipid subspecies are known to play important roles in Mθ mobility, phagocytosis, and apoptosis (Greenberg et al., 2006; Mariño and Kroemer, 2013; Shiratsuchi et al., 1998). Consistent with this, Lai and colleagues have recently reported that the absence of miR-33 in Mθs alters membrane microdomains, influencing the innate immune response (Lai et al., 2016). By overlaying our RNA-seq data with a network of genes known to interact with these lipid sub-species, we can identify a number of genes that are significantly dysregulated by the loss of miR-33. Further predictive analysis demonstrates that many of these changes are predicted based on the observed alterations in these lipids. Moreover, the overall changes in this gene set are predicted to result in an inhibition of inflammatory response. This analysis indicates the changes in these specific lipid classes may contribute to the overall phenotypes observed in these mice, including effects on pathways like inflammatory response that were largely independent of the overall changes in lipid content. Further work looking at how loss of miR-33 impacts lipid rafts, membrane fluidity, and the lipid composition of atherosclerotic plaques will provide additional insight into how these alterations may affect atherogenesis.

Overall, this work supports the promising therapeutic potential of miR-33 inhibitors for directly promoting the efflux of cholesterol from arterial Mθs, thereby limiting Mθ lipid accumulation and preventing further Mθ recruitment and activation. However, our findings also highlight the potential adverse effects of inhibiting miR-33 in other organs due to the obesity, IR, and hyperlipidemia observed in whole-body *miR-33*$^{-/-}$ animals. These findings provide much needed insight into the mechanisms by which miR-33 regulates atherosclerotic plaque formation and metabolic function and suggest that targeted inhibition of miR-33 within atherosclerotic plaques may provide a more viable therapeutic option for limiting atherosclerotic plaque formation as observed in our BMT experiments. Further work elucidating the specific mechanisms by which miR-33 regulates Mθ functions such as inflammation and efferocytosis, as well as whole-body effects on obesity and IR, will further aid in assessing the therapeutic potential of miR-33 inhibition.

EXPERIMENTAL PROCEDURES

Further details and an outline of resources used in this work can be found in the Supplemental Experimental Procedures. Briefly, RNA-seq was performed through the Yale Center for Genome Analysis using an Illumina HiSeq 2000 platform (1× 75-bp read length). Trimmed reads were aligned using TopHat2, and transcript abundances and differences were calculated using cuffdiff. Gene network and pathway analysis were carried out using Gene Set Enrichment Analysis software (Broad Institute), Qlucore Omics Explorer v.3.2 (Qlucore AB), and Ingenuity Pathway Analysis (Ingenuity Systems QIAGEN). Data were deposited in NCBI Gene Expression Omnibus (GEO: GSE103133). Animal studies were approved by the Institutional Animal Care and Use Committee of Yale University School of Medicine. WT C57BL/6 and *Ldlr*$^{-/-}$ mice were purchased from The Jackson Laboratory (Bar Harbor, ME, USA). Generation of *miR-33*$^{-/-}$ mice was accomplished with the assistance of Cyagen Biosciences. Establishment of the *miR-33b*^{KI} mouse model was accomplished in collaboration with Ingenious Targeting Laboratory. Accelerated atherosclerosis was induced by feeding mice for 12 weeks with a western diet (WD) containing 1.25% cholesterol (D12108; Research Diets, New Brunswick, NJ, USA). BM transplant experiments, plaque characterization, measurements of metabolic function and of circulating and cellular lipids, and RCT were carried out using established techniques. Statistical differences were measured using an unpaired two-sided Student's t test or a one-way ANOVA with Bonferroni correction for multiple comparisons. Normality was checked using the Kolmogorov-Smirnov test. A nonparametric test (Mann-Whitney) was used when data did not pass the normality test. A value of $p < 0.05$ was considered statistically significant.

SUPPLEMENTAL INFORMATION

Supplemental Information includes Supplemental Experimental Procedures and seven figures and can be found with this article online at https://doi.org/10.1016/j.celrep.2017.10.023.

AUTHOR CONTRIBUTIONS

N.L.P. and C.F.-H. conceived and designed the study and wrote the manuscript. N.L.P., N.R., A.C.-D., X.Z., P.P., N.A., J.M., M.M., A.B., D.A.F., and Y.S. performed experiments and analyzed data.

ACKNOWLEDGMENTS

This work was supported by grants from the NIH (R35HL135820 to C.F.-H., R01HL105945 and R01HL135012 to Y.S., R01HL107794 to A.B., and F32DK10348902 to N.L.P.), the American Heart Association (16EIA27550005 to C.F.-H., 16GRNT26420047 to Y.S., and 17SDG33110002 to N.R.), the American Diabetes Association (1-16-PMF-002 to A.C.-D.), and the Foundation Leducq Transatlantic Network of Excellence in Cardiovascular Research, MIRVAD (to C.F.-H.). We would like to thank Sameet Mehta and Rolando

Garcia Milian for their assistance with the processing and analysis of RNA-seq data.

Received: June 14, 2017
Revised: September 12, 2017
Accepted: October 5, 2017
Published: October 31, 2017

REFERENCES

Allen, R.M., Marquart, T.J., Albert, C.J., Suchy, F.J., Wang, D.Q., Ananthanarayanan, M., Ford, D.A., and Baldán, A. (2012). miR-33 controls the expression of biliary transporters, and mediates statin- and diet-induced hepatotoxicity. EMBO Mol. Med. *4*, 882–895.

Allen, R.M., Marquart, T.J., Jesse, J.J., and Baldán, A. (2014). Control of very low-density lipoprotein secretion by N-ethylmaleimide-sensitive factor and miR-33. Circ. Res. *115*, 10–22.

Ambros, V. (2004). The functions of animal microRNAs. Nature *431*, 350–355.

Bartel, D.P. (2009). MicroRNAs: target recognition and regulatory functions. Cell *136*, 215–233.

Barwari, T., Joshi, A., and Mayr, M. (2016). MicroRNAs in cardiovascular disease. J. Am. Coll. Cardiol. *68*, 2577–2584.

Dávalos, A., Goedeke, L., Smibert, P., Ramírez, C.M., Warrier, N.P., Andreo, U., Cirera-Salinas, D., Rayner, K., Suresh, U., Pastor-Pareja, J.C., et al. (2011). miR-33a/b contribute to the regulation of fatty acid metabolism and insulin signaling. Proc. Natl. Acad. Sci. USA *108*, 9232–9237.

Fernández-Hernando, C., Suárez, Y., Rayner, K.J., and Moore, K.J. (2011). MicroRNAs in lipid metabolism. Curr. Opin. Lipidol. *22*, 86–92.

Fernández-Hernando, C., Ramírez, C.M., Goedeke, L., and Suárez, Y. (2013). MicroRNAs in metabolic disease. Arterioscler. Thromb. Vasc. Biol. *33*, 178–185.

Gerin, I., Clerbaux, L.A., Haumont, O., Lanthier, N., Das, A.K., Burant, C.F., Leclercq, I.A., MacDougald, O.A., and Bommer, G.T. (2010). Expression of miR-33 from an SREBP2 intron inhibits cholesterol export and fatty acid oxidation. J. Biol. Chem. *285*, 33652–33661.

Goedeke, L., Vales-Lara, F.M., Fenstermaker, M., Cirera-Salinas, D., Chamorro-Jorganes, A., Ramírez, C.M., Mattison, J.A., de Cabo, R., Suárez, Y., and Fernández-Hernando, C. (2013). A regulatory role for microRNA 33* in controlling lipid metabolism gene expression. Mol. Cell. Biol. *33*, 2339–2352.

Goedeke, L., Salerno, A., Ramírez, C.M., Guo, L., Allen, R.M., Yin, X., Langley, S.R., Esau, C., Wanschel, A., Fisher, E.A., et al. (2014). Long-term therapeutic silencing of miR-33 increases circulating triglyceride levels and hepatic lipid accumulation in mice. EMBO Mol. Med. *6*, 1133–1141.

Greenberg, M.E., Sun, M., Zhang, R., Febbraio, M., Silverstein, R., and Hazen, S.L. (2006). Oxidized phosphatidylserine-CD36 interactions play an essential role in macrophage-dependent phagocytosis of apoptotic cells. J. Exp. Med. *203*, 2613–2625.

Horie, T., Ono, K., Horiguchi, M., Nishi, H., Nakamura, T., Nagao, K., Kinoshita, M., Kuwabara, Y., Marusawa, H., Iwanaga, Y., et al. (2010). MicroRNA-33 encoded by an intron of sterol regulatory element-binding protein 2 (Srebp2) regulates HDL in vivo. Proc. Natl. Acad. Sci. USA *107*, 17321–17326.

Horie, T., Baba, O., Kuwabara, Y., Chujo, Y., Watanabe, S., Kinoshita, M., Horiguchi, M., Nakamura, T., Chonabayashi, K., Hishizawa, M., et al. (2012). MicroRNA-33 deficiency reduces the progression of atherosclerotic plaque in *ApoE*$^{-/-}$ mice. J. Am. Heart Assoc. *1*, e003376.

Horie, T., Nishino, T., Baba, O., Kuwabara, Y., Nakao, T., Nishiga, M., Usami, S., Izuhara, M., Sowa, N., Yahagi, N., et al. (2013). MicroRNA-33 regulates sterol regulatory element-binding protein 1 expression in mice. Nat. Commun. *4*, 2883.

Horie, T., Nishino, T., Baba, O., Kuwabara, Y., Nakao, T., Nishiga, M., Usami, S., Izuhara, M., Nakazeki, F., Ide, Y., et al. (2014). MicroRNA-33b knock-in mice for an intron of sterol regulatory element-binding factor 1 (Srebf1) exhibit reduced HDL-C in vivo. Sci. Rep. *4*, 5312.

Horton, J.D., Goldstein, J.L., and Brown, M.S. (2002). SREBPs: activators of the complete program of cholesterol and fatty acid synthesis in the liver. J. Clin. Invest. *109*, 1125–1131.

Karunakaran, D., Thrush, A.B., Nguyen, M.A., Richards, L., Geoffrion, M., Singaravelu, R., Ramphos, E., Shangari, P., Ouimet, M., Pezacki, J.P., et al. (2015). Macrophage mitochondrial energy status regulates cholesterol efflux and is enhanced by anti-miR33 in atherosclerosis. Circ. Res. *117*, 266–278.

Lai, L., Azzam, K.M., Lin, W.C., Rai, P., Lowe, J.M., Gabor, K.A., Madenspacher, J.H., Aloor, J.J., Parks, J.S., Näär, A.M., and Fessler, M.B. (2016). MicroRNA-33 regulates the innate immune response via ATP binding cassette transporter-mediated remodeling of membrane microdomains. J. Biol. Chem. *291*, 19651–19660.

Lewis, G.F., and Rader, D.J. (2005). New insights into the regulation of HDL metabolism and reverse cholesterol transport. Circ. Res. *96*, 1221–1232.

Li, A.C., Binder, C.J., Gutierrez, A., Brown, K.K., Plotkin, C.R., Pattison, J.W., Valledor, A.F., Davis, R.A., Willson, T.M., Witztum, J.L., et al. (2004). Differential inhibition of macrophage foam-cell formation and atherosclerosis in mice by PPARalpha, beta/delta, and gamma. J. Clin. Invest. *114*, 1564–1576.

Li, T., Francl, J.M., Boehme, S., and Chiang, J.Y. (2013). Regulation of cholesterol and bile acid homeostasis by the cholesterol 7α-hydroxylase/steroid response element-binding protein 2/microRNA-33a axis in mice. Hepatology *58*, 1111–1121.

Mariño, G., and Kroemer, G. (2013). Mechanisms of apoptotic phosphatidylserine exposure. Cell Res. *23*, 1247–1248.

Marquart, T.J., Allen, R.M., Ory, D.S., and Baldán, A. (2010). miR-33 links SREBP-2 induction to repression of sterol transporters. Proc. Natl. Acad. Sci. USA *107*, 12228–12232.

Marquart, T.J., Wu, J., Lusis, A.J., and Baldán, Á. (2013). Anti-miR-33 therapy does not alter the progression of atherosclerosis in low-density lipoprotein receptor-deficient mice. Arterioscler. Thromb. Vasc. Biol. *33*, 455–458.

Najafi-Shoushtari, S.H., Kristo, F., Li, Y., Shioda, T., Cohen, D.E., Gerszten, R.E., and Näär, A.M. (2010). MicroRNA-33 and the SREBP host genes cooperate to control cholesterol homeostasis. Science *328*, 1566–1569.

Ouimet, M., Ediriweera, H.N., Gundra, U.M., Sheedy, F.J., Ramkhelawon, B., Hutchison, S.B., Rinehold, K., van Solingen, C., Fullerton, M.D., Cecchini, K., et al. (2015). MicroRNA-33-dependent regulation of macrophage metabolism directs immune cell polarization in atherosclerosis. J. Clin. Invest. *125*, 4334–4348.

Ouimet, M., Ediriweera, H., Afonso, M.S., Ramkhelawon, B., Singaravelu, R., Liao, X., Bandler, R.C., Rahman, K., Fisher, E.A., Rayner, K.J., et al. (2017). microRNA-33 regulates macrophage autophagy in atherosclerosis. Arterioscler. Thromb. Vasc. Biol. *37*, 1058–1067.

Poller, W., Dimmeler, S., Heymans, S., Zeller, T., Haas, J., Karakas, M., Leistner, D.M., Jakob, P., Nakagawa, S., Blankenberg, S., et al. (2017). Non-coding RNAs in cardiovascular diseases: diagnostic and therapeutic perspectives. Eur. Heart J. Published online April 18, 2017. https://doi.org/10.1093/eurheartj/ehx165.

Rader, D.J., and deGoma, E.M. (2014). Future of cholesteryl ester transfer protein inhibitors. Annu. Rev. Med. *65*, 385–403.

Rader, D.J., and Hovingh, G.K. (2014). HDL and cardiovascular disease. Lancet *384*, 618–625.

Rayner, K.J., Suárez, Y., Dávalos, A., Parathath, S., Fitzgerald, M.L., Tamehiro, N., Fisher, E.A., Moore, K.J., and Fernández-Hernando, C. (2010). MiR-33 contributes to the regulation of cholesterol homeostasis. Science *328*, 1570–1573.

Rayner, K.J., Esau, C.C., Hussain, F.N., McDaniel, A.L., Marshall, S.M., van Gils, J.M., Ray, T.D., Sheedy, F.J., Goedeke, L., Liu, X., et al. (2011a). Inhibition of miR-33a/b in non-human primates raises plasma HDL and lowers VLDL triglycerides. Nature *478*, 404–407.

Rayner, K.J., Sheedy, F.J., Esau, C.C., Hussain, F.N., Temel, R.E., Parathath, S., van Gils, J.M., Rayner, A.J., Chang, A.N., Suarez, Y., et al. (2011b). Antagonism of miR-33 in mice promotes reverse cholesterol transport and regression of atherosclerosis. J. Clin. Invest. *121*, 2921–2931.

Rosenson, R.S., Brewer, H.B., Jr., Davidson, W.S., Fayad, Z.A., Fuster, V., Goldstein, J., Hellerstein, M., Jiang, X.C., Phillips, M.C., Rader, D.J., et al.

(2012). Cholesterol efflux and atheroprotection: advancing the concept of reverse cholesterol transport. Circulation *125*, 1905–1919.

Rotllan, N., Ramírez, C.M., Aryal, B., Esau, C.C., and Fernández-Hernando, C. (2013). Therapeutic silencing of microRNA-33 inhibits the progression of atherosclerosis in *Ldlr*$^{-/-}$ mice—brief report. Arterioscler. Thromb. Vasc. Biol. *33*, 1973–1977.

Rottiers, V., Obad, S., Petri, A., McGarrah, R., Lindholm, M.W., Black, J.C., Sinha, S., Goody, R.J., Lawrence, M.S., deLemos, A.S., et al. (2013). Pharmacological inhibition of a microRNA family in nonhuman primates by a seed-targeting 8-mer antimiR. Sci. Transl. Med. *5*, 212ra162.

Shiratsuchi, A., Osada, S., Kanazawa, S., and Nakanishi, Y. (1998). Essential role of phosphatidylserine externalization in apoptosing cell phagocytosis by macrophages. Biochem. Biophys. Res. Commun. *246*, 549–555.

Tall, A.R., Yvan-Charvet, L., Terasaka, N., Pagler, T., and Wang, N. (2008). HDL, ABC transporters, and cholesterol efflux: implications for the treatment of atherosclerosis. Cell Metab. *7*, 365–375.